Derivation of Stiffness Matrices for Modeling a Human Cervical Spine

Antonio J. Flores Zavala* and Young Eun Kim**

(Received October 8, 1993)

Based on the published experimental data under static loading condition, stiffness matrices of the cervical spine were developed. These matrices simulate well the static response of the cervical spine as shown by the authors in an earlier work, while for a dynamic simulation these matrices need some modifications in order to achieve more accurate results. We present a method, in the form of a constrained optimization problem, that facilitates the evaluation of the stiffness matrices to be used in a dynamic simulation. The intervertebral disk and the ligaments are represented by an equivalent stiffness matrix whose elements are assumed to be constant over the entire range of mobility. With a set of new stiffness matrices derived by the proposed method, the dynamic simulation showed a good agreement with the observed motion data.

Key Words: Cervical Spine, Stiffness Matrix, Monte Carlo Method, Transfer Matrix Method, Standard Deviation, Dynamic Motion

1. Introduction

The significance of motion simulation models as research tools in contributing to physiological research on human cervical spine has been recognized by many investigators. The mechanical characteristics of the passive components of the cervical spine can be accurately quantified in-vitro by measuring the relation between loads appied to cervical spine and its resultant displacement.

Several researches have reported on the load-displacements characteristics of functional spinal units(FSU), which defined as two adjacent vertebrae and intervening soft tissues, usually under static conditions.

Panjabi, et al.(1976) applied a load in one direction to the upper thoracic vertebra of a FSU that had the lower vertebra rigidly attached to the base of a testing apparatus and then measured its resulting displacements. The displacement in the load direction divided by the magnitude of the load gives the main flexibility coefficient, while the others displacements divided by that load give the coupling flexibility coefficients for that motion. Following the same procedure, they derived three-dimensional flexibility properties of the human thoracic spine. Deng and Goldsmith(1987), using anatomical considerations, modified these matrices and used them for the dynamic analysis of the cervical spine. McElhaney, et al.(1988) used a combined bending and axial loading for evaluating the stiffness which revealed the anisotropic and nonlinear behavior. They also concluded that the bending stiffness of the cervical spine was significantly influenced by the direction of the bending moment, the types of the imposed restraints, the magnitude of the deformation and the deformation history. Nightingale, et al.(1991) analysed the influence of the end conditions on the cervical spine injury mechanisms and on the stiffness. They stated that, within a given specimen, the imposition of different end conditions to the cervical spine results in large changes in the observed axial stiffness.

*Graduate School, Dankook University
**Deptartment of Mechanical Engineering, Dankook University

Pintar, et al.(1990) worked with entire cervical spine. They applied an axial loading to the cervical spine and measured the resulting deformations in the entire cervical spine. This data gives an idea about the total displacement of the cervical spine at each level. Myers, et al.(1989) gave date for the passive torsional response of the entire human cervical spine. The rotational stiffness was measured after a rotation of 66.8 degrees from the neutral position. Panjabi, et al.(1988) evaluated the three-dimensional movements of the occipito-atlanto-axial joint complex, quantifying the neutral zone(zone of displacements at a very small load) and the elastic zone. Flexibility coefficients for the occiput-C1 and C1-C2 joints were also derived.

The mechanical response of the FSU is both nonlinear and time dependent, this implies that the load-displacement relation changes for diffe rent applied forces and rates of loading. This is one of the reasons for the discrepancy in the published results. Differences in experimental technique may be responsible for some variations in collected data.

Edwards, et al.(1987) calculated the stiffness of lumbar FSU using the Least Square Method by minimizing the quadratic error between the expe rimentally applied loads and the estimated loads based on the calculated stiffness. They used symmetric matrices for getting a set of six equations that solve for six distinct coefficients used to describe the planar motion. This consideration do not reflect a nonlinear, time dependent load-displacement relation. Laborde, et al.(1981) presented experimental non-symmetric matrices reflecting a load-displacement relation with nonlinear, time dependent characteristics. The measured coupling coefficients showed the asymmetry of the matrix. Moroney, et al.(1988) reported the principal and coupled motions of cervical segments and also did a statistical analysis. Panjabi, et al.(1976), (1986), (1988) and Patwardhan, et al. (1982) measured the flexibility matrix and then by matrix inversion calculated the stiffness matrix. Usually the investigators did not measure the complete 3-D flexibility matrix ; so, in simulating a 3-D motion it is needed to assemble these matrices using data from several sources. Due to the coupling terms in stiffness matrix it is difficult to combine data from different researchers and then satisfy all the experimental results. The best compromise is to use the main motions and its range of motion for getting a 3-D flexibility matrix that can be used for obtaining results close to the experimental ones.

In our earlier research(1992), simulation results under static loading condition showed a good agreement with experimental data. Despite nume rous studies of quasistatic response of the FSU at low loads, relatively little is known about the mechanics of the cervical spine at other rate of loading, especially at dynamic loading. Moreover, the diversity of the published experimental data, the use of an stiffness matrix obtained under static loading condition obligate us to make some modification to the stiffness matrices for dynamic modeling of the cervical spine.

The goal of this study is to present a method for obtaining the optimal stiffness characteristics of the cervical motion segments using experimental data from different sources in order to make an accurate dynamic simulation of the cervical spine. The Transfer Matrix Method(TMM) in combination with optimization method was employed to calculate the stiffness matrices and the response of the human head and cervical spine to direct head impact.

2. Stiffness Calculation by an Optimization Analysis

The estimated stiffness coefficients were calculated by inverting the flexibility matrix and minimizing the quadratic error between the displacements obtained from the stiffness relation and the actual experimental data. The ranges of motion were used as constraints.

The problem can be announced as

$$\text{Min } F_i=(\delta_i-u_i)^2 \tag{1}$$

subjected to

$$\delta_{1i}\leq \boldsymbol{u}_i\leq \delta_{2i} \tag{2}$$

where F_i=objective functions

δ_i=experimental displacements

u_i=calculated displacements
i=number of coupling coefficients for a specified motion
δ_{1i}=lower limit of range of motion
δ_{2i}=upper limit of range of motion

For solving the problem it is used a multicrite rion optimization analysis in which the goal is to minimize not a single objective function but several functions simultaneously. The Monte Carlo Method, in which a certain number of points are picked at random over the estimated range of all the variables, is used as a function minimization. Then the Pareto optimal solutions are evaluated using the following concept:

A point $x^* \in X$ is Pareto optimal if for every x(vector of decision variables) $\in X$(n-dimensional Euclidean space of variables) either

$$F_i(x)=F_i(x^*)$$
$$i=1, \cdots k \text{ objective functions}$$

or there is at least one i such that

$$F_i(x)>F_i(x^*) \quad i=1, \cdots k$$

This definition is based upon the intuitive conviction that the point x^* is chosen as the optimal if no criterion can be improved without worsening at least another criterion.

The minimum of the function is determined by inspection. From this set of solutions the min-optimal solution is chosen using the Min-Max aproach. This optimum is described as follows. Knowing the extremes of the objective functions the desirable solution is the one which gives the smallest value of the relative increments of all the objective functions with respect to their extremes.

The difference between the flexibility coefficients or stiffness coefficients published by several authors is reduced by considering its standard deviations. Depending on the statistical probabi lity curve an evaluation criterion can be chosen. For example, 68.3 per cent of all items fall within one standard deviation on each side of mean. This criterion is considered in imposing the optimization constraints. The mean displacements are considered for evaluating the objectives functions.

In Figure 1, an algorithm for getting the optimal flexibility matrix is described

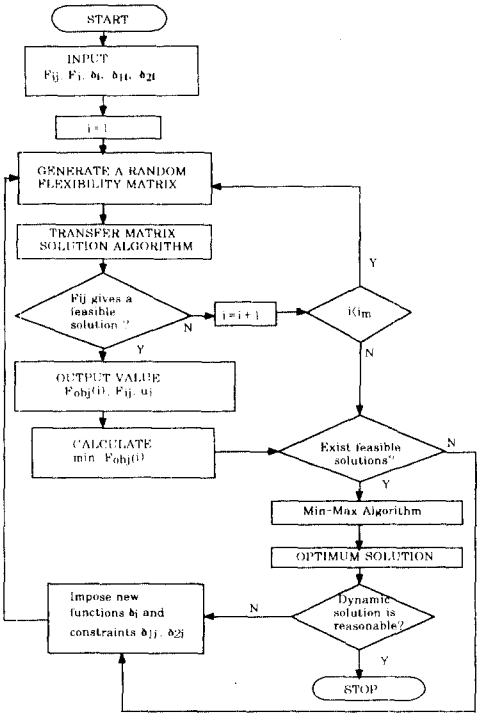

Fig. 1 Flow chart of the optimization

3. The Transfer Matrix Method

Consider the general element of Fig. 2. The force vector P, and displacement vector D are expressed by

$$P_{i-1}=[S_1, S_2, S_3, S_4, S_5, S_6]^T \quad (3)$$
$$P_i=[S_7, S_8, S_9, S_{10}, S_{11}, S_{12}]^T \quad (4)$$
$$D_{i-1}=[u_1, u_2, u_3, u_4, u_5, u_6]^T \quad (5)$$
$$D_i=[u_7, u_8, u_9, u_{10}, u_{11}, u_{12}]^T \quad (6)$$

Physiologically speaking, the negative force vector is formed by compression($-S_7$), posterior shear ($-S_8$), right lateral shear($-S_9$), right axial rotation($-S_{10}$), left lateral bending($-S_{11}$) and extension($-S_{12}$).

The state vector of bending, torsion and axial components in the vertebral mass center $i-1$ of an arbitrary element k, that is, kth FSU of the discrete simulation is given by

$$[Q]_k=[u_1(i-1), u_2(i-1), u_3(i-1), u_4(i-1), u_5(i-1), u_6(i-1), S_1(i-1), S_2(i-1), S_3(i-1), S_4(i-1), S_5(i-1), S_6(i-1), 1]_k \quad (7)$$

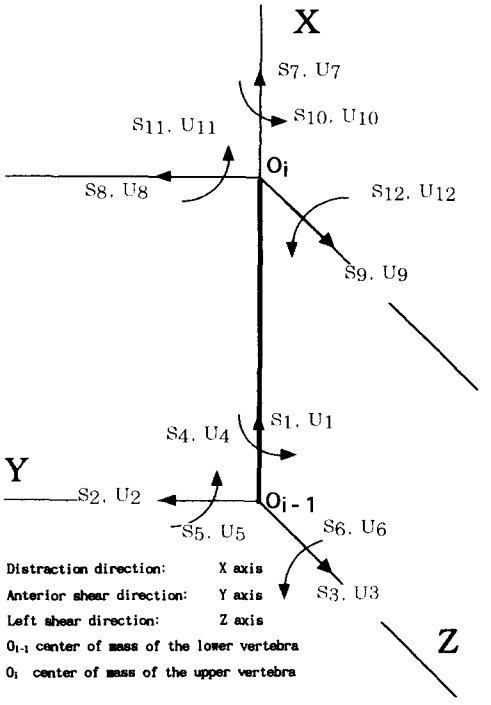

Fig. 2 Coordinate system

The force-deformation relation for the element k is defined by

$$\begin{bmatrix} P_i \\ P_{i-1} \end{bmatrix}_k = \begin{bmatrix} A & B \\ C & D \end{bmatrix} \begin{bmatrix} D_i \\ D_{i-1} \end{bmatrix}_k \tag{8}$$

Expanding Eq. (8) and solving for the state vector at the vertebral mass center i as a function of the state vector at the vertebral mass center $i-1$ of the analysed element we get

$$\begin{bmatrix} D_i \\ P_i \end{bmatrix}_k = \begin{bmatrix} -C^{-1}D & C^{-1} \\ B-AC^{-1}D & AC^{-1} \end{bmatrix} \begin{bmatrix} D_{i-1} \\ S_{i-1} \end{bmatrix}_k = BK \begin{bmatrix} D_{i-1} \\ S_{i-1} \end{bmatrix}_k \tag{9}$$

where BK is called the Transfer Matrix of the analysed element.

For the $(k+1)$th FSU, we have

$$\begin{bmatrix} D_{i-1} \\ P_{i-1} \end{bmatrix}_{k+1} = CK \begin{bmatrix} D_i \\ P_i \end{bmatrix}_k \tag{10}$$

The Nodal Matrix CK, incorporates inertial parameters, prescribed deformations, slopes, moments, etc.

After continuous multiplication of the transfer and nodal matrices BK, CK, we obtain the relation between the state vectors at the two ends of the model, that is, vertebra T_1 and head.

$$[Q]_{head} = [CBK][Q]_{T1} \tag{11}$$

where

$$[CBK] = [CK]_9[BK]_8[CK]_8 [BK]_8[BK]_{n-2}[CK]_{n-2}, \cdots [BK]_1.$$

After incorporating the boundary conditions, Eq. (11) will give a set of simultaneous equations. The number of these equations is as same as that of the unknown state variables in $[Q]_1$, then these variables can be found by solving these equations.

Once the initial state vector $[Q]_1$ is known in vertebra T_1 the determination of the state vectors in each vertebral mass center are obtained by successive multiplication of transfer matrices and nodal matrices ; this operation is expressed by

$$[Q]_m = \sum_{i=1}^{m-1} [CK]_{i+1}[BK]_i[Q]_1 \tag{12}$$

or

$$[Q]_2 = [CK]_2[BK]_1[Q]_1$$
$$[Q]_3 = [CK]_3[BK]_2[Q]_2$$
$$\vdots$$

Time response problems can be solved with a direct time integration scheme.

For time equal $t+\theta\Delta t$, we have

$$\bar{K}(t)\, U_{t+\theta\Delta t} = \bar{P}_{t+\theta\Delta t} \tag{13}$$

where the effective stiffness matrix is given by

$$\bar{K}(t) = K(t) + A_0 M + A_1 C \tag{14}$$

The modified load $\bar{P}(t)$ is given by

$$\bar{P}_{t+\theta\Delta t} = P_t + \theta(P_{t+\theta\Delta t} - P_t) + M(A_0 U_t + A_2 \dot{U}_t + 2\ddot{U}_t) + C(A_1 U_t + 2\dot{U}_t + A_3 \ddot{U}_t) \tag{15}$$

At time $t+\Delta t$ we get

$$\ddot{U}_{t+\Delta t} = A_4(U_{t+\theta\Delta t} - U_t) + A_5 \dot{U}_t + A_8 \ddot{U}_t \tag{16}$$

$$\dot{U}_{t+\Delta t} = \dot{U}_t + A_7(\ddot{U}_{t+\Delta t} + \ddot{U}_t) \tag{17}$$

$$U_{t+\Delta t} = U_t + \Delta t \dot{U}_t + A_8(\ddot{U}_{t+\Delta t} + 2\ddot{U}_t) \tag{18}$$

Where M is the lumped mass ; C the damping coefficient, θ, A_0, A_1, A_2, A_3, A_4, A_5, A_6, A_7, A_8 are integration parameters from the Wilson method of direct time integration. Using Eqs. (14) and (15) in Eq. (13) and identifying Eq. (13) as Eq. (8), we will be working in the general algor-

ithm of the transfer matrix method and evaluate $U_{t+\theta\Delta t}$ with the value of $U_{t+\theta\Delta t}$, the values of $\ddot{U}_{t+\Delta t}$, $\dot{U}_{t+\Delta t}$ and $U_{t+\Delta t}$ are evaluated for any time step Δt.

4. Evaluation Process

For computing the optimal stiffness coe ffiecients first we obtained the experimental flexibility coefficients following the procedure described by Panjabi(1976). Then, by using an optimization criterion the optimal stiffness coefficients can be obtained. The procedure are listed as follows ;

Applied load : S_j
Measure resulting displacements : δ_i
Main motion : $i=j$
Coupled motion : $i\neq j$
Average displacements : $\overline{\delta_i}$
Range of motions : δ_{1i}, δ_{2i}
Calculate flexibility coeff. :

$$F_{ij}=\frac{\delta_{opt(i)}}{S_j}$$

$\delta_{1i}<\delta_{opt(i)}<\delta_{2i}$
control parameter : $\overline{\delta_i}$
Calculate stiffness matrix :by inversion of the flexibility matrix.

Calculate the transfer matrix$[BK]_1$: use Eq. (9)

Repeat the same procedure for all the cervical vertebrae for finding the transfer matrices that will transfer the state vector through the complete model. That is, $[BK]_2$, $[BK]_3$, $[BK]_4$, ···

Incorporating the transfer matrices $[BK]_i$, the nodal matrices $[CK]_i$, the inertial parameters and boundary conditions into the algorithm of the transfer matrix a complete simulation of the dynamic behavior of the cervical spine is obtained

An example is given next.

Applied anterior shear load S(2) : 100 N.
Resulting displacements : $\overline{\delta_1}$, $\overline{\delta_2}$, $\overline{\delta_6}$

Displacements obtained from simulation :

$$u_1,\ u_2,\ u_6$$

$$\text{Min } F(1)=(\overline{\delta_1}-u_1)^2 \tag{19a}$$
$$F(2)=(\overline{\delta_2}-u_2)^2 \tag{19b}$$
$$F(3)=(\overline{\delta_6}-u_6)^2 \tag{19c}$$

subjected to :

$$\delta_{11}<u_1<\delta_{21} \tag{20a}$$
$$\delta_{12}<u_2<\delta_{22} \tag{20b}$$
$$\delta_{16}<u_6<\delta_{26} \tag{20c}$$

Table 1 illustrates the experimental data used in the simulation. Table 2 includes the constraints and the main motions used in the objective func-

Table 1 Experimental flexibility data used in simulation

Author	Load	Main motion	Range of motion	Coupled motion	Range of motion	Coupled motion	Range of motion
Shea, et al. (1991)	Compression at 500 N	F_{11} 8.98E−07	1.22E−06 7.08E−07	F_{21} 6.75E−07	9.17E−07 5.32E−07	F_{61} 3.52E−05	4.78E−05 2.77E−05
	Posterior Shear at 100 N	F_{22} 8.70E−06	1.03E−05 7.52E−06	F_{12} 2.35E−07	2.78E−07 2.03E−07	F_{62} 4.10E−05	4.86E−05 3.55E−05
	Extension at 3.5 Nm	F_{66} 7.62E−03	2.00E−02 4.68E−03	F_{16} 1.12E−05	2.93E−05 6.86E−06	F_{26} 1.44E−04	3.77E−04 8.83E−05
Moroney, et al. (1988)	Right Lateral Shear at 19.6 N	F_{33} 8.40E−06	3.57E−05 4.42E−06	F_{43} 1.88E−04	8.00E−04 9.91E−05	F_{53} 1.15E−04	4.89E−04 6.05E−05
	Left Bending at 1.8 Nm	F_{55} 2.57E−02	9.18E−02 1.10E−02	F_{35} 1.50E−04	5.37E−04 6.43E−05	F_{45} 8.19E−03	2.90E−02 3.50E−03
Myers, et al. (1989)	Right AxialRotation	F_{44} 4.62E−03	6.71E−03 3.52E−03	F_{34} 5.57E−05	8.08E−05 4.24E−05	F_{54} 2.37E−03	3.45E−03 1.81E−03

Units : m/N, rad/Nm

Table 2 Constraints values used in optimization problem.

Applied Load S2:	100 N		
Mean Displacement (m)	$\overline{\delta_1}$ −0.0000232	$\overline{\delta_2}$ −0.000850	$\overline{\delta_6}$ −0.004200
Upper Constraint (m)	δ_{21} −0.000020	δ_{22} −0.000752	δ_{26} −0.003550
Lower Constraint (m)	δ_{11} −0.000028	δ_{12} −0.001030	δ_{16} −0.004860
Simulated Displacement (m)	u_1 −0.000022	u_2 −0.000793	u_6 −0.00395

Table 3 Minimum of the objective functions

Function minimization	F(1)	F(2)	F(3)
First minimization	1.10E−12	3.69E−09	6.674E−08
Second minimization	7.34E−12	2.59E−09	1.377E−07
Third minimization	6.25E−12	5.18E−09	4.278E−08
Extreme of the objective functions $F(i)^0$	1.10E−12	2.59E−09	4.278E−08

Table 4 Results of the optimization procedure

	Function values			Relative deviations		
Optimal solutions	F(1)	F(2)	F(3)	⊿F(1)	⊿F(2)	⊿F(3)
1	1.17E−12	3.14E−09	1.048E−07	5.91E−02	2.15E−01	1.45E+00
2	5.74E−12	3.13E−09	1.043E−07	4.20E+00	2.09E−01	1.44E+00
3	4.26E−12	5.78E−09	4.971E−08	2.85E+00	1.23E+00	1.61E−01
4	4.51E−12	2.84E−09	3.946E−07	3.08E+00	9.71E−02	8.22E+00
5	5.29E−12	3.31E−09	5.106E−08	3.79E+00	2.80E−01	1.93E−01
6	5.85E−12	2.90E−09	1.614E−07	4.30E+00	1.20E−01	2.77E+00
7	6.25E−12	5.18E−09	4.278E−07	4.66E+00	1.00E+00	0.00E+00
8	1.19E−12	3.28E−09	6.218E−08	8.15E−02	2.67E−01	4.53E−01
9	1.10E−12	3.69E−09	6.674E−08	0.00E+00	4.26E−01	5.60E−01
10	7.34E−12	2.59E−09	1.376E−07	5.64E+00	0.00E+00	2.22E+00
11	2.49E−12	3.97E−09	6.090E−08	1.26E+00	5.35E−01	4.23E−01
12	2.35E−12	3.05E−09	1.300E−07	1.13E+00	1.78E−01	2.04E+00
Final solution	1.19E−12	3.28E−09	6.218E−08	8.15E−02	2.67E−01	4.53E−01

tions ($\overline{\delta_1}$, $\overline{\delta_2}$, $\overline{\delta_6}$).

The output of the function minimization is given in Table 3.

A set of optimal solutions is calculated on the base of the Pareto optimum. The min-max optimum compares relative deviations of each objective function from the minima $F(i)^0$ given in Table 3. For the ith objective function of any set of optimal solutions the relative deviation is calculated by

$$\Delta F(i)=\frac{|F(i)-F(i)^0|}{F(i)^0} \tag{21}$$

The relative deviations are given in Table 4.

The min-max solution chooses from each set the maximum ΔF, then makes a comparison between all the maxima ΔF from all the sets and chooses the minimum ΔF. The set for which belongs the minimum ΔF is the solution.

5. Results and Discussion

Using the coordinate system illustrated in Fig. 2, the stiffness matrix for the $C2-C3$, $C3-C4$, $C4-C5$ vertebrae is given by

$$K=\begin{bmatrix} 149.100 & 3.127 & 0.000 & 0.000 & 0.000 & -0.199 \\ 0.928 & 13.910 & 0.000 & 0.000 & 0.000 & -0.254 \\ 0.000 & 0.000 & 29.490 & 0.491 & 0.249 & 0.000 \\ 0.000 & 0.000 & 0.959 & 0.047 & -0.016 & 0.000 \\ 0.000 & 0.000 & 0.272 & -0.008 & 0.009 & 0.000 \\ -0.924 & -0.094 & 0.000 & 0.000 & 0.000 & 0.024 \end{bmatrix} \times 10^4$$

(*Unit* : N, m, rad.)

In obtaining this matrix we used the data measured by Moroney, et al.(1988) Shea, et al. (1991) and Myers, et al.(1989). The values are given in Table 1 ; these values correspond to loads of high magnitude, region where the stiffness matrices are relatively linear. Shea, et al. suggested the modeling of the cervical spine as three distinct mobile regions $C1-C2$, $C2-C5$, $C5-T1$; regions for which we have calculated therespectivestiffnessmatrices($C1-C2$; $C2-C3$, $C3-C4$, $C4-C5$; $C5-C6$, $C6-C7$, $C7-T1$) together with the matrix for Head$-C1$. The stiffness of the functional spinal units is not constant over the range of physiological loads. Panjabi used low loads while our matrices were built using high applied loads that are close to the strength limit as is the case in an automobile accident. In evaluating the motions, we gave the same importance to the main and coupling motions which are specified in the objective functions ; after 100 iterations we got a deviation of 5.45%, 7.18% and 6.33%, for $\overline{\delta_1}$, $\overline{\delta_2}$ and $\overline{\delta_6}$ respectively.

Usually in simulating the dynamic behavior of the spine, the published stiffness values lead to an unreasonable results. This is mainly due to the use of experimental stiffness data assembled from different researchers under conditions distinct to the actual ones. Our new method will help to estimate the stiffness matrix that could lead to obtain realistic results. Once the unreasonable variables are localized, we work with the stiffness matrices for estimating new variable values ; that is, imposing new functions or constraints we will create a new stiffness matrix, which should be matched with the data on hand. Williams and Belytschko(1983) followed a similar procedure in the early stages of constructing their head-neck model for impact studies, however they did not used a systematic procedure. In order to show the application of these concepts we present a dynamic analysis that can be used for analyzing the influence of the stiffness matrices in the modeling of the human spine.

With the measurement of forces and displacements in the entire spine and individual intervertebral segments, it is possible to obtain three-dimensional stiffness properties, including coupling effects that simulate accurately the mechanical response of the spine in each level. We will get a set of functions for each level of the spine with the respective constraints, and the minimization

will be done for the entire spine simultaneously.

In case of dynamic simulation, impact force of 3850 N was applied to the center of gravity of the head in the anterior-posterior direction($-S7$). The force profile is of triangular shape acting during 5 ms with the highest magnitude at 2.5 ms. Damping is not considered in this analysis. Same physical and geometrical properties of the Deng and Goldsmith(1987) were used in dynamic ana lysis. Figures 3, 4 and 5 shows the displacements, velocities, and accelerations of the center of gravity of the head with respect to the first thoracic vertebra($T1$) respectively. Our results have a good correlation, with a in-vitro experiments performed by Huston(1975). The velocity and acceleration of the model at the beginning of the simulation have the same pattern with the experimental values, however the numerical results are higher than the experimental ones. This discrepancy is believed to be mainly due to the existence of the so called neutral zone ; in this region large displacements take place for small applied

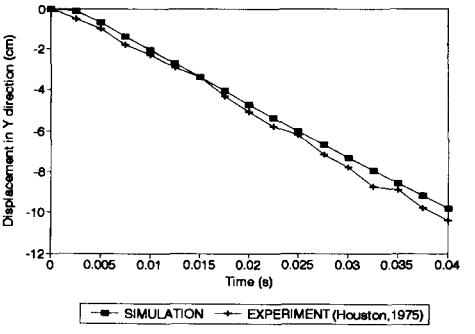

Fig. 3 Displacement of head in Y direction

loads which usually is not reported in some cases and combined with the elastic zone in others. For more accurate results both zones should be distinguished and considered in the modeling. Another reason for these disagreements may be the no consideration of the nonlinearity due to facet joint contact.

The stiffness matrices for several spinal segments that were used for the motion simulation of the human cervical spine are listed as follows.

Stiffness matrix for Head$-C1$ vertebra

$$K=\begin{bmatrix} 240.9000 & 5.3840 & 0.0000 & 0.0000 & 0.0000 & -0.2462 \\ 0.5136 & 22.9400 & 0.0000 & 0.0000 & 0.0000 & -0.4395 \\ 0.0000 & 0.0000 & 2748.0000 & 48.7200 & 31.1000 & 0.0000 \\ 0.0000 & 0.0000 & 0.0991 & 0.0035 & -0.0016 & 0.0000 \\ 0.0000 & 0.0000 & 0.1054 & -0.0029 & 0.0032 & 0.0000 \\ -0.0175 & -0.0018 & 0.0000 & 0.0000 & 0.0000 & 0.0005 \end{bmatrix} \times 10^4$$

Stiffness matrix for $C1-C2$ vertebrae

$$K=\begin{bmatrix} 269.4000 & 5.6860 & 0.0000 & 0.0000 & 0.0000 & -0.3009 \\ 5.0500 & 39.5600 & 0.0000 & 0.0000 & 0.0000 & -0.7099 \\ 0.0000 & 0.0000 & 80.0700 & 1.4760 & 0.9646 & 0.0000 \\ 0.0000 & 0.0000 & 0.0132 & 0.0005 & -0.0002 & 0.0000 \\ 0.0000 & 0.0000 & 0.1553 & -0.0045 & 0.0051 & 0.0000 \\ -0.0331 & -0.0038 & 0.0000 & 0.0000 & 0.0000 & 0.0009 \end{bmatrix} \times 10^4$$

Stiffness matrix for $C5-C6$; $C6-C7$; $C7-T1$ vertebrae

$$K=\begin{bmatrix} 95.1300 & 1.8870 & 0.0000 & 0.0000 & 0.0000 & -0.1858 \\ 12.0500 & 19.2500 & 0.0000 & 0.0000 & 0.0000 & -0.7470 \\ 0.0000 & 0.0000 & 48.6100 & 0.9320 & 0.5840 & 0.0000 \\ 0.0000 & 0.0000 & 1.9050 & 0.0705 & -0.0347 & 0.0000 \\ 0.0000 & 0.0000 & 0.6200 & -0.0170 & 0.0169 & 0.0000 \\ -0.6474 & -0.0681 & 0.0000 & 0.0000 & 0.0000 & 0.0200 \end{bmatrix} \times 10^4$$

(*Units* : *N. m. rad.*)

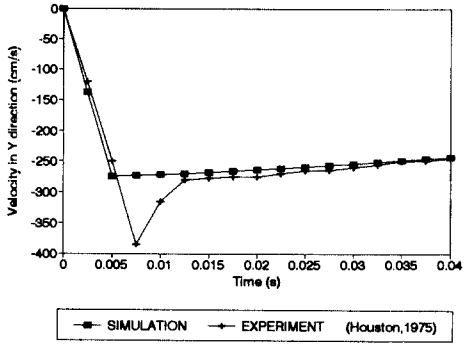

Fig. 4 Velocity of head in Y direction

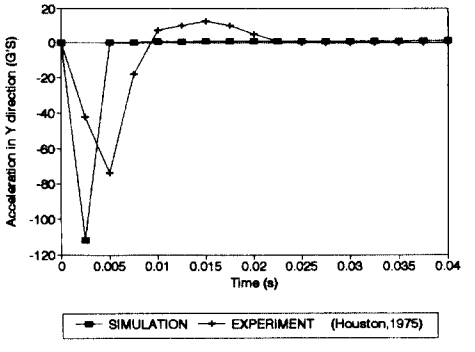

Fig. 5 Acceleration of head in Y direction

6. Conclusion

The stiffness matrices obtained from experimental data using the Monte Carlo Method in combination with Transfer Matrix Method simulates accurately the cervical spine behavior under an impact loading condition. For getting results closer to the experimental ones the stiffness coefficients can be changed under certain limits, which are given by the range of motion and statistical considerations. When it is applied to the cervical spine modeling, the Transfer Matrix Method in combination with a direct time integration scheme, proves to be a powerful method of analysis. The TMM uses matrices of relatively small order and has short computational time, which could allow the modeling of the complete human spine incorporating stiffness matrices for several load levels.

AcKnowledgement

This work was supported by KOSEF grant 921-0900-016-2

References

Deng, Y. C. and Goldsmith, W., 1987, "Response of a Human Head/Neck/Upper-Torso Replica to Dynamic Loading-II. Analytical Model," Journal of Biomechanics, Vol. 20, pp. 487~497.

Edwards, W. T., Hayes, W. C., Posner, I., White III, A. A. and Mann, R. W., 1987, "Variation of Lumbar Spine Stiffness with Load," Journal of Biomechanical Engineering, Vol. 109, pp. 35~42.

Flores, Z. A. and Kim, Y. E., 1992, "State Vector Transfer in the Cervical Vertebral Motion Under Static Load," SAE No. 923951, pp. 488~496.

Goel, V. K., Clark, C. R., Harris, K. G., Kim, Y. E. and Schulte, K. R., 1989, "Evaluation of Effectiveness of a Facet Wiring Technique : An in Vitro Biomechanical Investigation" Annals of Biomedical Engineering, Vol. 17, pp. 115~126.

Huston, J. C., 1975, "A Comprehensive Ana lysis of Head and Dynamics Arising from Impact and Inertia Forces," Ph. D. Thesis, West Virginia University, West Virginia.

Laborde, J. M., Burstein, A. H., Song, K., Brown, R. H. and Bahniuk, E., 1981, "A Method of Analyzing the Three-Dimensional Stiffness Properties of the Intact Human Lumbar Spine," Journal of Biomechanical Engineering, Vol. 103, pp. 299~300.

McElhaney, J. H., Doherty, B. J., Paver, J. G., Myers, B. S. and Gray, L., 1988, "Combined Bending and Axial Loading Responses of the Human Cervical Spine," Proc. 32nd Stapp Car Crash Conf., Society Automotive Engineers, Warrendale, PA, pp. 21~28.

Moroney, S. P., Schultz, A. B., Miller, J. A. A. and Andersson, G. B. J., 1988, "Load-Displacement Properties of Lower Cervical Spine Motion Segments," Journal of Biomechanics, Vol.

21, pp. 769~779.

Myers, B. S., McElhaney, J. H., Doherty B. J., Paver, J. G., Nightingale, R. W., Ladd, T. P. and Gray, L., 1989, "Response of the Human Cervical Spine to Torsion," Proc. 33rd Stapp Car Crash Conference, pp. 215~222.

Nightingale, R. W., Doherty, B. J., Myers, B. S., McElhaney, J. H. and Richardson, W. J., 1991, "The Influence of End Conditions on Human Cervical Spine Injury Mechanisms," Proc. 35rd Stapp Car Crash Conf., Society of Automotive Engineers, Warrendale, PA, pp. 391~399.

Osyczka, A., 1984, "Multicriterion Optimization in Engineering," John Wiley & Sons, Toronto.

Panjabi, M. M., Brand, R. A. and White III, A. A., 1976, "Three-Dimensional Flexibility and Stiffness Properties of the Human Thoracic Spine," Journal of Biomechanics Vol. 9, pp. 185~192.

Panjabi, M. M., Summers, D. J., Pelker, R. R., Videman, T., Friedlaender, G. E. and Southwick, W. O., 1986, "Three-Dimensional Load-Displacement Curves Due to Forces on the Cervical Spine," Journal of Orthopaedic Research, Vol.4, pp. 152~161.

Panjabi, M. M., Dvorak, J., Duranceau, J., Yamamoto, I., Gerber, M., Wolfgang, R. and Bueff, H. U., 1988, "Three-Dimensional Movements of the Upper Cervical Spine," Spine, Vol. 13, pp. 726~730.

Patrick, Y. L., Bishop, J., Wells, R. P. and McGill, S. M., 1991, "A Quasi-Static Analytical Sagittal Plane Model of the Cervical Spine in Extension and Compression," Proc. 35rd Stapp Car Crash Conf., Society of Automotive Engineers, Warrendale, PA, pp. 419~433.

Patwardhan, A. G., Soni, A. H., Sullivan, J. A., Gudavalli, M. R. and Srinivasan, V., 1982, "Kinematic Analysis and Simulation of Vertebral Motion Under Static Load-Part II : Simulation Study," Journal of Biomechanical Engineering, Vol. 104, pp. 112~118.

Pintar, F. A., Sances, Jr. A., Yoganandan, N., Reinartz, J., Maiman, D., Suh, J. K., Unger, G., Cusick, J. F. and Larson, S. J., 1990, "Biodynamics of the Total Human Cadaveric Cervical Spine," Proc. 34th Stapp Car Crash Conference, pp. 55~72.

Shea, M., Edwards, W. T., White, A. A. and Hayes, W. C., 1991, " Variations of Stiffness and Strength Along the Human Cervical Spine," Journal of Biomechanics, Vol. 24, pp. 95~107.

Vanderby, R., Daniele, M., Patwardhan, A. and Bunch, W., 1986, "A Method for the Identification of In-Vivo Segmental Stiffness Pro perties of the Spine," Journal of Biomechanical Engineering. Vol. 108, pp. 312~316.

Williams, J. L. and Belytschko, T. B., 1983, "A Three-Dimensional Model of the Human Cervical Spine for Impact Simulation," Journal of Biomechanical Engineering, Vol. 105, pp. 321~331.